International Journal of Engineering Research & Technology (IJERT)
ISSN: 2278-0181
Vol. 15 Issue 04 , April - 2026

Optimization of Distribution Power Grid Operation using Branch Current Model Method

Dinh-Dang Nguyen
Faculty of Electrical and Electronics Engineering,
Nha Trang College of Technology, Khanh Hoa, Vietnam

Abstract. The power loss on the distribution grid (DG) has always accounted for a high proportion of the total power loss of the system because it is operated at low voltage levels. Therefore, reducing the loss of capacity during the operation of the DG is important. This article presents the method of choosing the optimum operating structure to reduce power loss based on optimum branch current modeling methods. The results of the evaluation of the effectiveness of the methods were carried out on the IEEE 33 node and the IEEE 69 nodes grid using the PSS/ADEPT software.

Keywords. Distribution grid, power loss, optimal branch current model, IEEE 33 node, IEEE 69 node system, PSS/ADEPT.

1. INTRODUCTION

Power loss is an inherent and significant issue in electrical power systems, particularly within distribution grids (DGs). This loss accounts for a high proportion of the total system power loss, primarily because DGs operate at low voltage levels. Therefore, minimizing power loss during DG operation is a crucial objective, not only from a technical standpoint but also economically, to enhance the efficiency and reliability of the power system.

In recent years, the problem of minimizing power losses through distribution network reconfiguration has attracted considerable attention. This problem can generally be approached using two main categories of methods: metaheuristic and heuristic approaches.

Metaheuristic methods are optimization algorithms inspired by natural processes and phenomena, which have demonstrated strong capabilities in solving complex nonlinear problems. Common algorithms in this category include Genetic Algorithms (GA) [6], [14]–[16], Particle Swarm Optimization (PSO) [17]–[22], [29], and other swarm-based or evolutionary techniques. These methods are widely adopted due to their flexibility and ability to avoid local optima.

In contrast, heuristic methods rely on practical rules, operator experience, and domain-specific knowledge acquired through the actual operation of power systems [7]–[13]. Although often simpler in structure and less computationally intensive, heuristic methods can offer effective solutions in many practical applications.

Among the heuristic approaches, two methods stand out due to their simplicity and applicability in real-world operation: the Optimal Branch Current Model 1 (OBCMM_1) and Optimal Branch Current Model 2 (OBCMM_2). OBCMM_1, introduced in [10], transforms the original distribution network with complex impedance into a purely resistive network. Power flow calculations are then performed on this resistive closed-loop network to sequentially determine open switches, gradually achieving a radial topology. Meanwhile, OBCMM_2, proposed in [11], performs load flow analysis on a purely resistive network containing a single loop, iteratively replacing the initially open switch with an alternative one to reach the desired radial configuration.

This paper evaluates the effectiveness of the OBCMM_1 and OBCMM_2 methods for distribution network reconfiguration (DNR) with the objective of minimizing power losses. Their performance is compared against the topology-based method (TOPO) to identify the most optimal operating configuration.

The evaluation is conducted on standard 33- node and 69-node distribution test systems. Unlike previous studies that assume purely resistive networks, this study considers networks with complex impedance. The simulations are carried out with the support of PSS/ADEPT 5.0, enabling more realistic modeling of power flow and switch operation.

International Journal of Engineering Research & Technology (IJERT)
ISSN: 2278-0181
Vol. 15 Issue 04 , April - 2026

2. THEORETICAL BASIS OF DISTRIBUTION GRID OPERATION

2.1. Radial Distribution Grid Analysis

Radial distribution grids are common structures in distribution systems, where branches are connected in a tree-like fashion without closed loops. Figure 2.1 illustrates the structural diagram of a radial distribution grid.

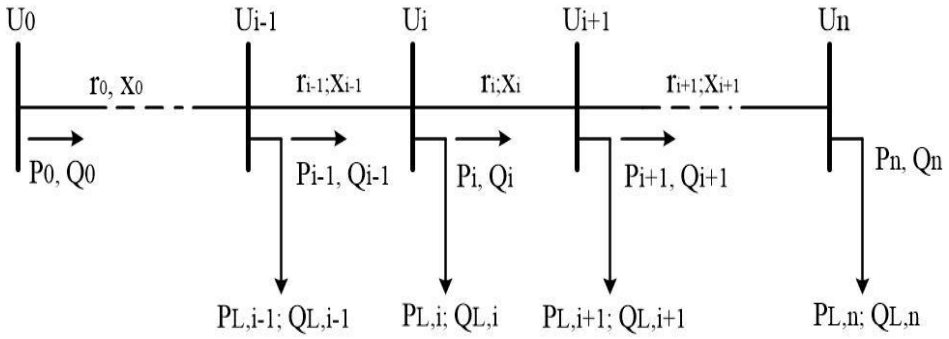

Figure 2.1 Diagram of radial distribution grids

The key variables in radial grid analysis include:

n: Number of branches.

U_0: Voltage at the balance node (source node).

U_i: Voltage at branch nodes (i = 1, 2,..., n).

r_i, x_i: Resistance and reactance of the i-th branch.

P_i, Q_i: Active power and reactive power on the branches.

P_{Li}, Q_{Li}: Active and reactive power loads at the i-th node.

- To calculate and determine power loss on the current. Replace the current with the following alternative diagram:

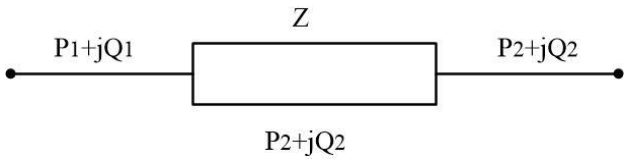

Figure 2.2 Distribution current replacement diagram

To calculate and determine power loss in the current, the current is represented by an equivalent circuit diagram as depicted in Figure 2.2. The total circuit impedance is defined as Z = R + jX.

Equation (2.1) quantifies the active power loss in the current as:

$$\Delta P = 3I^2R = \frac{S^2}{U_{dm}^2}R = \frac{P_2^2 + Q_2^2}{U_{dm}^2}R \quad (2.1)$$

Assuming $U_i = U_{đm}$ and $U_{đm} = 1$, Equation (2.1) can be simplified to Equation (2.2):

$$\Delta P = 3I^2R = S^2R = P_2^2R + Q_2^2R \quad (2.2)$$

This equation allows for efficient calculation of power loss under certain assumed conditions.

2.2 Characteristics of Closed-Loop Distribution Grids and Power Loss

International Journal of Engineering Research & Technology (IJERT)
ISSN: 2278-0181
Vol. 15 Issue 04 , April - 2026

A closed-loop distribution grid is established when an initially open switch within a radial distribution network is closed, thereby forming a loop. Figure 2.3 illustrates the diagram of a closed-loop distribution grid with branch XY initially as an open switch. When the switch on branch XY is closed, the original radial grid becomes a closed grid.

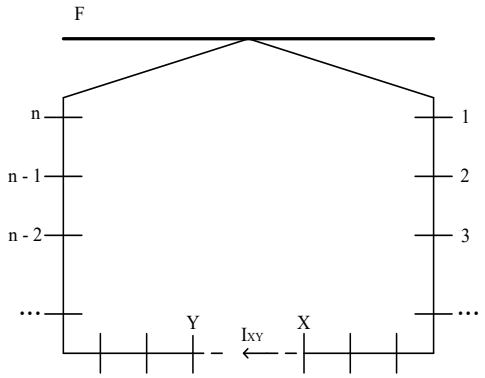

Figure 2.3 Diagram of a closed-loop distribution grid

The power loss of the system when operating in a closed-loop mode is determined by Equation (2.3):

$$Ploss_{closed} = \sum_{i=1}^{N_{FX}} R_i I_i^2 + \sum_{j=1}^{N_{FY}} R_j I_j^2 + R_{XY} I_{XY}^2 \quad (2.3)$$

Where N_{FX} and N_{FY} are the branches from source F to X and from source F to Y, respectively. R_{XY} and I_{XY} are the resistance and current flowing through branch XY.

When unlocked on the XY branch, the grid becomes a ray grid. At this time, it can be seen that the current on the FX branch (I_{XY}) will decrease by an amount and the current on the FY branch (I_{XY}) will increase by an amount. The loss on the DG with open XY branch is determined by the expression:

$$Ploss_{open} = \sum_{i=1}^{N_{FX}} R_i (I_i - I_{XY})^2 + \sum_{j=1}^{N_{FY}} R_j (I_j + I_{XY})^2 \quad (2.4)$$

Then, we have the loss deviation when switching from closed operation to open operation determined [6], [29]:

$$Ploss_{open} - Ploss_{closed} = I_{XY}^2 \left(\sum_{i=1}^{N_{FX}} R_i + R_{XY} + \sum_{j=1}^{N_{FY}} R_j \right) \quad (2.5)$$

From Equation (2.5), it can be observed that as the current IXY approaches 0 ($I_{XY} \rightarrow 0$), the loss deviation between the open and closed grids also approaches 0 ($Ploss_{open}$ - $Ploss_{closed} \rightarrow 0$). This implies that when $I_{XY} = 0$, the losses in the open grid will be equal to the losses in the closed grid.

A critical inference from this analysis is that within a closed-loop distribution grid, when operating in an open configuration (by opening a switch on a specific branch), if the current flowing through that branch is minimal, the resulting radial grid structure will exhibit the lowest power losses. This provides a strong theoretical basis for optimal branch current model algorithms, justifying their approach of identifying and opening switches with the smallest currents to achieve an optimal configuration. This is not merely a formula but a core principle explaining why these algorithms focus on opening switches with minimum current, ensuring that these methods are built upon the physical laws of power flow.

International Journal of Engineering Research & Technology (IJERT)
ISSN: 2278-0181
Vol. 15 Issue 04 , April - 2026

2.3. Overview of Power Loss Reduction Methods in Distribution Grids (DG)

To reduce power loss in distribution grids, various reconfiguration methods have been studied and developed, primarily falling into two groups: heuristic and meta-heuristic methods.

- Heuristic method: These methods are predicated on empirical knowledge and practical insights derived from power system operation. Merlin and Back (1975) proposed reconfiguration to reduce power loss, combining optimization and heuristics to determine an operating configuration with minimal power loss while ensuring the distribution system maintains a radial structure [30]. Shirmohammadi and Hong [10] introduced another modification to the original algorithm by Merlin and Back, utilizing a heuristic approach to describe power loss reduction through the opening and closing of switches [30]. Civanlar et al. proposed reconfiguring distribution equipment to minimize losses, exclusively employing heuristics in the DG restructuring process [8]. Rubin Taleski proposed a method to minimize the energy loss function, similar to Civanlar's approach but replacing the power loss function with an energy loss function, based on load diagrams and average voltage calculated over 24 hours [9]. C. S. Chen and M. Y. Cho developed a method to reduce energy loss by performing the opening and closing of critical switches, offering an optimal solution for both short-term and long-term operations of the distribution power system [12].

A common characteristic of heuristic methods is their independence from the continuity requirement of the objective function, offering computational efficiency and the potential to yield global optima. However, these methods have some limitations, such as the need for careful adjustment of parameters and the potential to get trapped in local optima.

- **Meta heuristic method:** These methods are optimization algorithms inspired by natural behaviors or evolutionary processes. Particle Swarm Optimization (PSO) Algorithm: This algorithm is based on the relationships, operational organization, and behavior within populations, such as flocks of birds searching for food or ant colonies finding their way back to the nest. PSO is applied in various fields, including function optimization, open control systems, neural networks, and wireless sensor networks [17, 22, 29]. Genetic Algorithm (GA): This algorithm is based on the processes of evolution, natural selection, and natural genetics, combining evolutionary processes with functional optimization. The selection of "good chromosomes" helps to provide effective solutions and ensures the convergence of the algorithm [6], [14-16].

While extensive research has focused on both categories of methods for power loss reduction, heuristic approaches are considered more accessible and effective in addressing constrained optimization problems without necessitating objective function continuity. This implies that for the problem of distribution grid reconfiguration, the simplicity and practical effectiveness of heuristic methods may outweigh the theoretical guarantees of global optimality offered by meta-heuristic methods, especially in the context of real-world operations. This section provides an important overview, clarifying why OBCMM methods (belonging to the heuristic group) were chosen for deeper investigation in this paper.

3. OPTIMAL BRANCH CURRENT MODEL METHODS FOR RECONFIGURATION

This study elaborates on the implementation steps for two methods based on the optimal branch current model, aimed at selecting the optimal radial operating structure.

3.1. Optimal Branch Current Model Method 1 (OBCMM_1)

The optimal branch current model method 1 (OBCMM_1) was proposed by Shirmohammadi and Hong [10]. The OBCMM_1 method begins by closing all normally open switches in a radial distribution network, thereby forming a meshed configuration. Branch impedances are then replaced with equivalent resistances, and power flow analysis is performed to identify the branch with the lowest current. The switch on this branch is opened to restore a radial structure while aiming to minimize power losses. This approach offers the advantage of simplifying complex combinatorial problems by leveraging operational experience, allowing for faster computation. Additionally, the final reconfiguration is independent of the initial mesh structure. However, for networks with a high number of switches, computation time can increase significantly due to the large number of loops. Moreover, because all loops are considered simultaneously during power flow distribution, complex interactions may prevent the identification of a globally optimal solution. The method also does not account for line or equipment losses, which may affect its practical accuracy. Sequence of Steps for OBCMM_1:

1. Step 1: Close all initially normally open electric switches; the grid becomes a closed grid.
2. Step 2: Perform power distribution for the grid and identify the branch with the smallest current.
3. Step 3: Open the electric switch in the closed loop that has the smallest current.

International Journal of Engineering Research & Technology (IJERT)
ISSN: 2278-0181
Vol. 15 Issue 04 , April - 2026

4. Step 4: Redistribute power to the grid.
5. Step 5: Continue repeating Step 3 until the grid is restored to a radial configuration.

The algorithm flowchart for OBCMM_1 is presented in Figure 3.1.

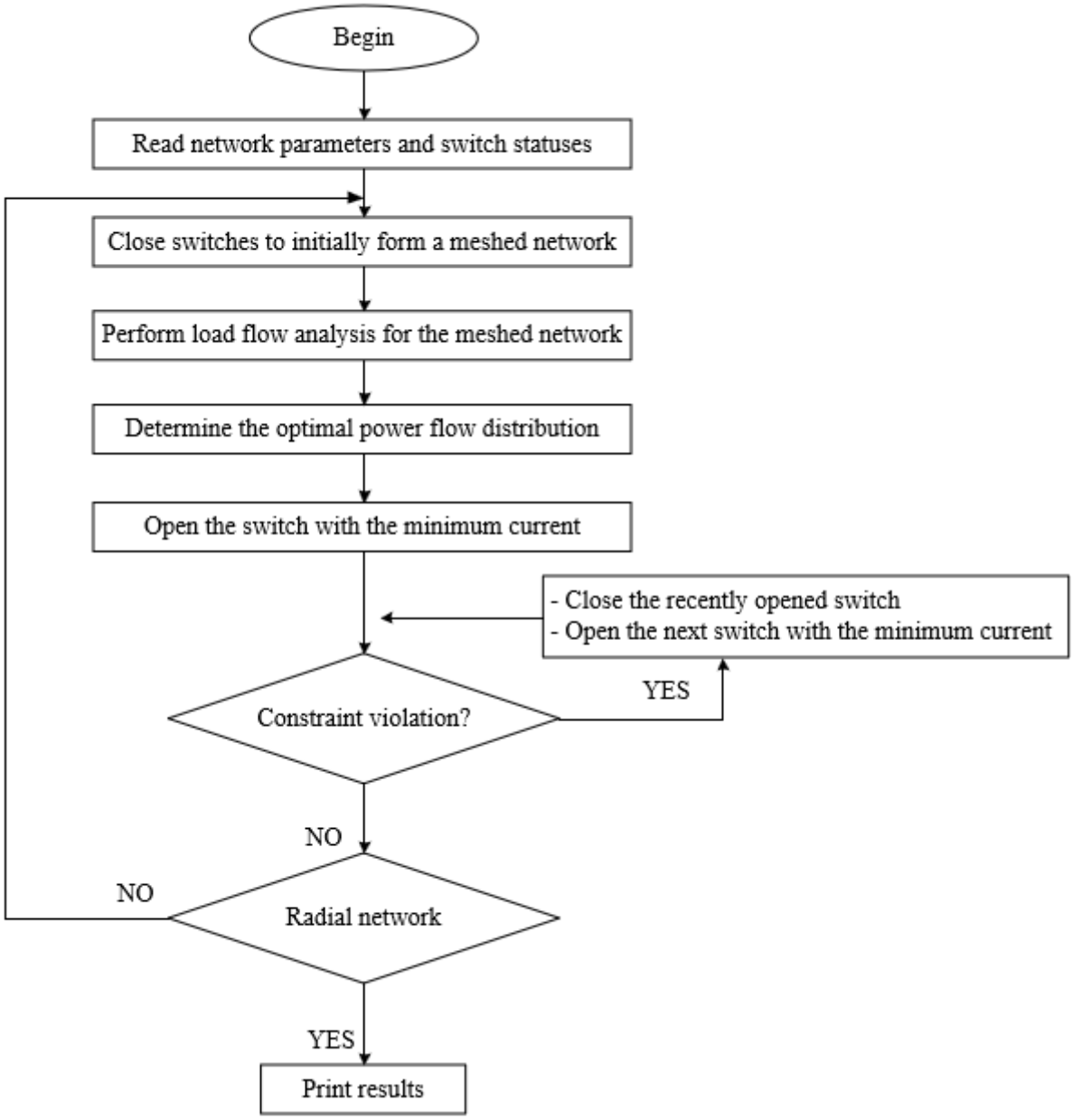

Figure 3.1 The algorithm flowchart for OBCMM_1

3.2. Optimal Branch Current Model Method 2 (OBCMM_2)

The Optimal Branch Current Model Method 2 (OBCMM_2) was proposed by S. K. Basu [11]. The OBCMM_2 method begins with a set of initially open switches. At each iteration, one open switch is closed to form a single loop within the original radial distribution network, while the remaining switches remain open. Power flow analysis is then conducted to identify the branch with the lowest current within the newly formed loop, and the corresponding switch is opened to restore the radial structure. This process is repeated sequentially for each initially open switch, with the goal of achieving a final configuration that minimizes power loss. A key advantage of this method is that it analyzes each loop independently, thereby eliminating inter-loop influences and potentially improving accuracy. However, its effectiveness is highly dependent on the order in which switches are closed and opened. A

International Journal of Engineering Research & Technology (IJERT)
ISSN: 2278-0181
Vol. 15 Issue 04 , April - 2026

suboptimal sequence may lead to local minima and prevent the attainment of a globally optimal solution. Furthermore, the iterative nature of the process can increase computational time in large networks. Sequence of steps to implement OBCMM_2 method:

Step 1: Close an electric lock in the initial set of open locks;

Step 2: Implement capacity allocation to the power grid;

Step 3: Open the electric lock in the closed loop with the smallest current to restore the ray-shaped grid;

Step 4: Close the next open electric lock in the initial set of opening locks;

Step 5: Implement capacity distribution for the power grid.

Step 6: Repeat step 3 until the last open electric lock in the original set of opening locks has been closed and replaced with a new electric lock.

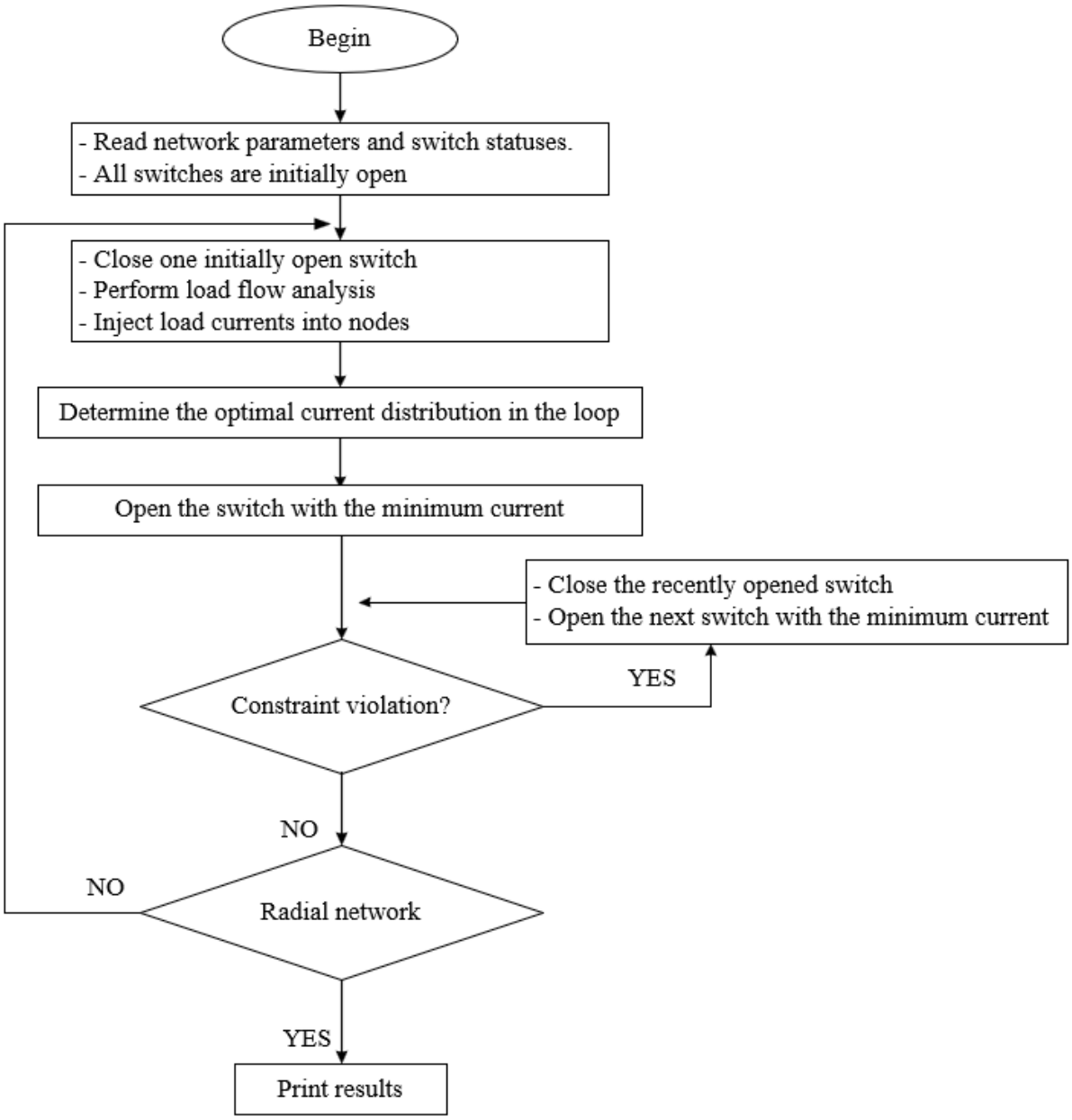

The algorithm flowchart for OBCMM_2 is presented in Figure 3.2.

Figure 3.2 The algorithm flowchart for OBCMM_2

International Journal of Engineering Research & Technology (IJERT)
ISSN: 2278-0181
Vol. 15 Issue 04 , April - 2026

The fundamental difference in how OBCMM_1 and OBCMM_2 handle loops (OBCMM_1 closes *all* open switches and gradually opens them, while OBCMM_2 closes *one switch at a time* to create a single closed loop and replaces it) is crucial. This explains their differing performance characteristics, particularly the "influence between loops" disadvantage of OBCMM_1 and the "dependence on initial order" of OBCMM_2. This difference represents a trade-off between global versus local optimization strategies within heuristic methods.

3.3. Tie Open Point Optimization (TOPO) Algorithm

The Tie Open Point Optimization (TOPO) algorithm is employed to determine optimal tie-open points, enabling the transformation of a meshed power grid into a radial configuration while minimizing power losses. This method is specifically designed for radial distribution systems, where the source node is typically treated as the root and used for calculations across multiple branches to achieve optimal results. The algorithm operates by sequentially closing open switches to form loops, solving the circuit to identify branches with minimal current, and selectively reopening switches to break the loops and restore radiality. Branches that do not form loops may be isolated or connected to separate networks. The process is repeated iteratively until a complete radial structure is achieved. Notably, the TOPO algorithm simplifies analysis by neglecting reactance, focusing instead on current flow magnitudes to guide switching decisions. The TOPO algorithm flowchart is presented in Figure 3.3.

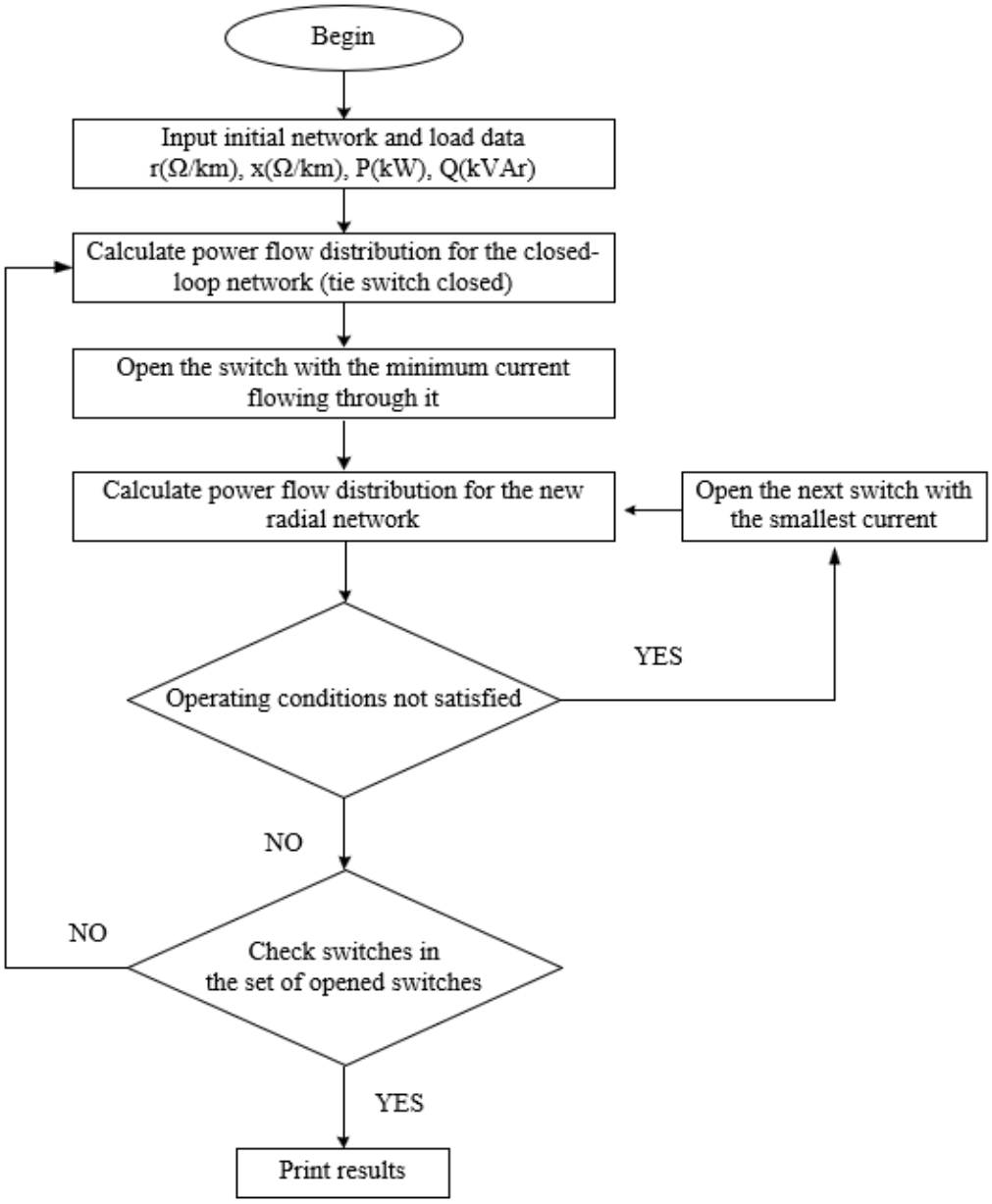

Figure 3.3 The TOPO algorithm flowchart

International Journal of Engineering Research & Technology (IJERT)
ISSN: 2278-0181
Vol. 15 Issue 04 , April - 2026

The use of TOPO as a benchmark, despite its disregard for reactance, indicates that it is considered a reliable, even "optimal" or near-optimal, method for loss reduction in radial systems under its simplifying assumptions. The paper's use of TOPO as a comparison point, even when OBCMM methods are tested with complex impedances, underscores TOPO's practical relevance in this field and provides a strong reference for validating the proposed methods.

4. EVALUATION RESULTS AND DISCUSSION

To assess the efficacy of the OBCMM_1 and OBCMM_2 methods, simulations were conducted on the standard IEEE 33-node and IEEE 69-node distribution test systems. It is assumed that losses associated with electrical equipment (transformers, switching devices) are negligible. The obtained results will be compared and verified using the Tie Open Point Optimization (TOPO) method with PSS/ADEPT software.

4.1. IEEE 33-Node Distribution Grid

The IEEE 33-node distribution grid has the following parameters: Voltage 12.66 kV. Total active power P = 3715kW, total reactive power Q = 2300 kVar. Load parameters for the branches are listed in Appendix 1.1, and line parameters in Appendix 1.2. The total number of branches is 37, with 32 normally closed electric switches and 5 initially normally open electric switches: SW33, SW34, SW35, SW36, SW37. The grid diagram is illustrated in Figure 4.1 and simulated using PSS/ADEPT 5.0 in Figure 4.2. Both OBCMM_1 and OBCMM_2 methods were implemented in PSS/ADEPT 5.0 software to select the optimal operating structure.

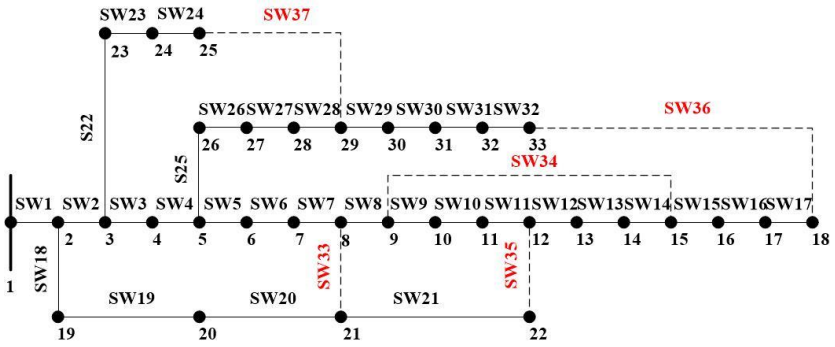

Figure 4.1 The grid diagram of IEEE 33-Node

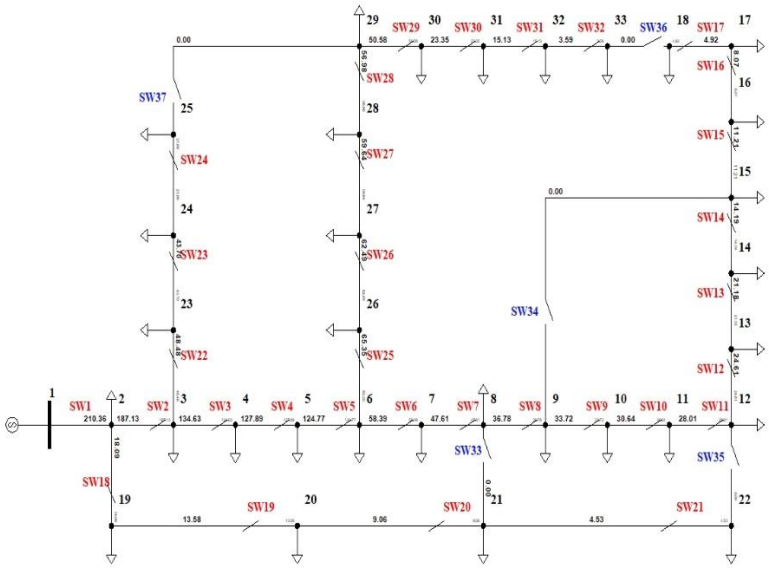

Figure 4.2 DG IEEE 33-Node simulated by using PSS/ADEPT 5.0

4.1.1. Application of OBCMM_1 Method (IEEE 33 nodes)

International Journal of Engineering Research & Technology (IJERT)
ISSN: 2278-0181
Vol. 15 Issue 04 , April - 2026

The results of detailed selection of the operating structure using the OBCMM_1 method are presented in Table 1. Upon closing all initially open switches and performing power flow analysis for the system, the OBCMM_1 method is applied. Considering the first closed loop, the branch containing electric switch SW7 has the smallest current of 11.35A, therefore, switch SW7 is opened. Power is then redistributed to the grid with SW7 open, and considering the second closed loop, switch SW9, which has the smallest current, is opened. This process is repeated until the 5th closed loop is considered. The final structure with open electric switches is {SW7, SW9, SW14, SW36, SW37}.

The initial power loss of the grid was ΔP_initial = 202.698 kW. After applying OBCMM_1, the power loss ΔP(OBCMM_1) = 142.163 kW, representing a reduction of 60.535 kW compared to the initial state, corresponding to a 29.864% decrease. Table 1 presents the detailed current calculation results for branches using OBCMM_1, and Table 2 along with Figures 4.3 and 4.4 show the node voltages after reconfiguration.

Table 1. Current results of calculating branches according to OBCMM_1 (IEEE 33 nodes)

Circulation	**Branch and current, respectively**							**Open lock**
1	Branch	**2**	**3**	**4**	**5**	**6**	**7**	**SW7**
	Current(A)	143.66	65.63	58.97	55.84	21.39	11.35	
	Branch	**18**	**19**	**20**	**33**			
	Current(A)	57.33	52.92	48.45	19.95			
2	Branch	**8**	**9**	**10**	**11**	**21**	**33**	**SW9**
	Current(A)	14.63	0.89	2.33	4.89	25.21	25.11	
	Branch	**35**						
	Current(A)	20.69						
3	Branch	**33**	**8**	**34**	**14**	**13**	**12**	**SW14**
	Current(A)	24.85	14.4	11.61	2.99	9.14	12.33	
	Branch	**35**	**21**					
	Current(A)	20.93	25.46					
4	Branch	**2**	**3**	**4**	**5**	**25**	**26**	**SW36**
	Current(A)	137.73	59.55	52.86	49.75	36.46	33.48	
	Branch	**27**	**28**	**29**	**30**	**31**	**32**	
	Current(A)	30.51	27.68	47.33	24.61	17.05	7.81	
	Branch	**36**	**17**	**16**	**15**	**34**	**8**	
	Current(A)	6.83	7.41	8.92	11.07	13.02	15.88	
	Branch	**33**	**20**	**19**	**18**			

International Journal of Engineering Research & Technology (IJERT)
ISSN: 2278-0181
Vol. 15 Issue 04 , April - 2026

	Current(A)	26.2	54.16	58.7	63.18			
5	Branch	**3**	**4**	**5**	**25**	**26**	**27**	**SW37**
	Current(A)	59.42	52.73	49.64	36.5	33.58	30.68	
	Branch	**28**	**37**	**24**	**23**	**22**		
	Current(A)	27.97	27.18	47.54	68.77	73.51		

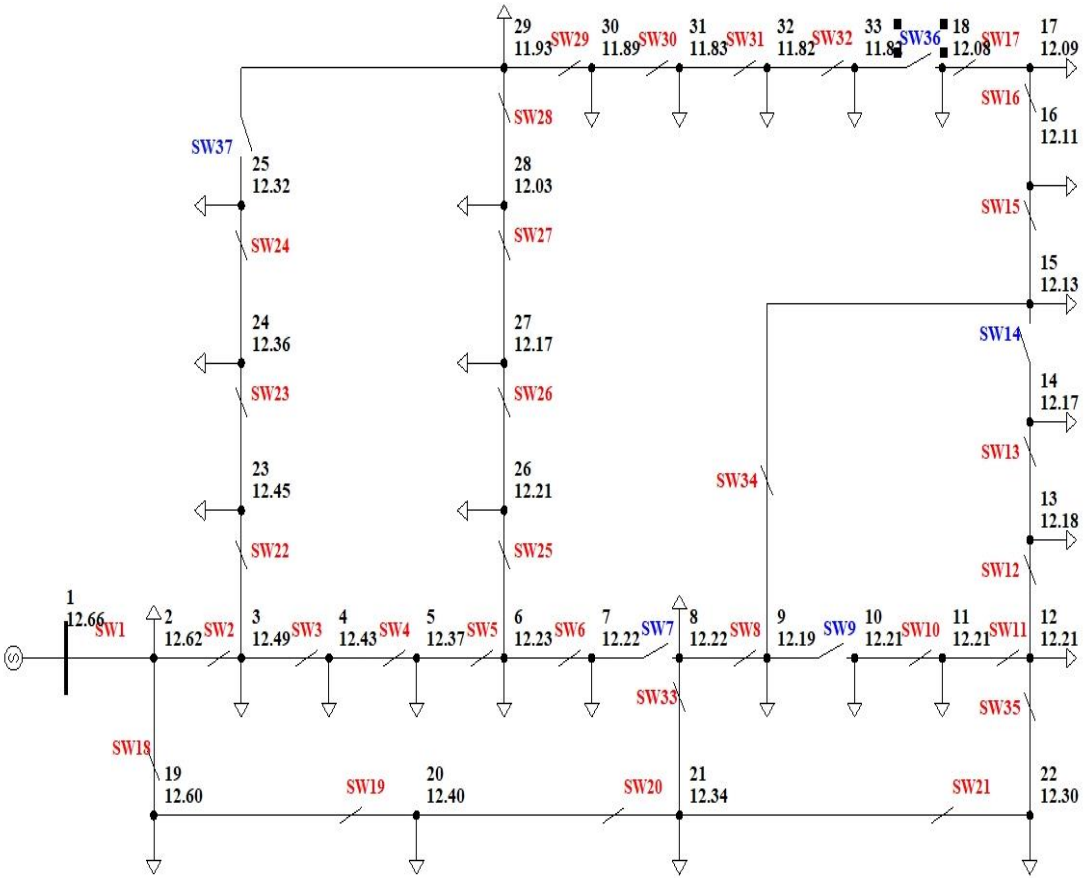

Figure 4.3 Node voltages according to ABC MM_1 (IEEE 33 nodes)

Table 2. Voltage amplitude values of OBCMM_1 nodes (IEEE 33 nodes)

Node	Voltage (kV)	Node	Voltage (kV)	Node	Voltage (kV)	Node	Voltage (kV)
1	12.66	10	12.21	18	12.08	26	12.21
2	12.62	11	12.21	19	12.6	27	12.17
3	12.49	12	12.21	20	12.40	28	12.03
4	12.43	13	12.18	21	12.34	29	11.93
5	12.37	14	12.17	22	12.30	30	11.89

International Journal of Engineering Research & Technology (IJERT)
ISSN: 2278-0181
Vol. 15 Issue 04 , April - 2026

6	12.23	15	12.13	23	12.45	31	11.83
7	12.22	16	12.11	24	12.36	32	11.82
8	12.22	17	12.09	25	12.32	33	11.82
9	12.19						

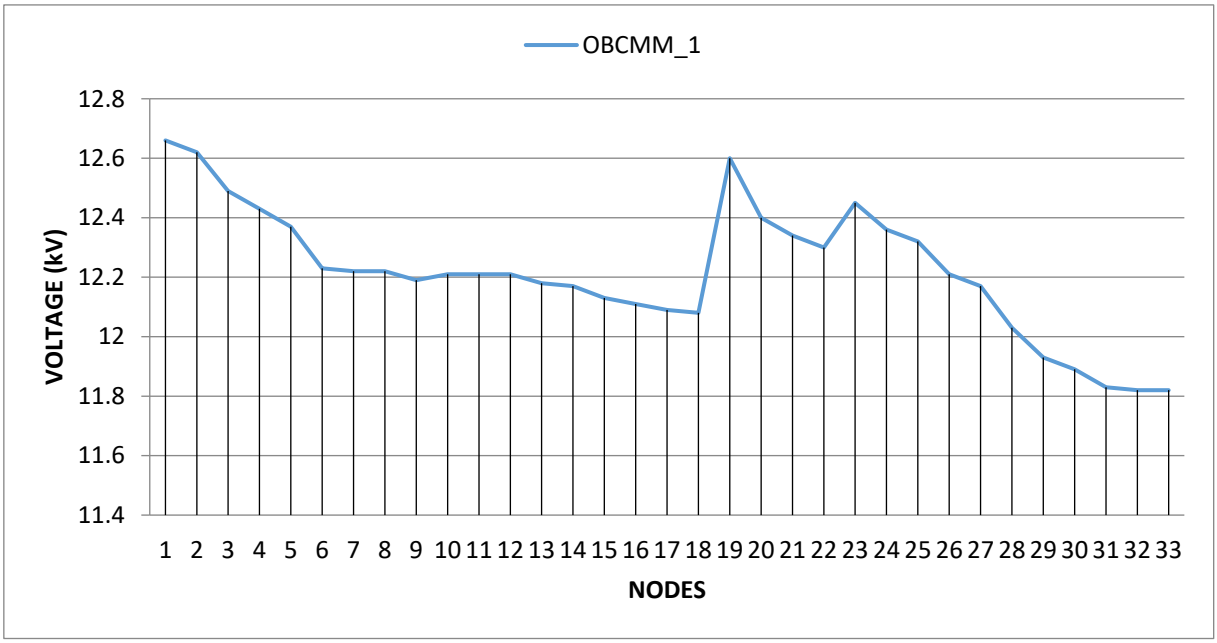

Figure 4.4 Voltage diagram of nodes after restructuring OBCMM_1 (IEEE 33 nodes)

4.1.2. OBCMM_2 method (IEEE 33 nodes)

The OBCMM_2 method was implemented by closing switch SW33 initially and performing power flow analysis for the resulting closed-loop grid (as switches SW34, SW35, SW36, SW37 remained open). The branch containing electric switch SW7 has the smallest current of 14.44A, therefore, switch SW7 is opened. Power is then redistributed to the grid with SW7 open, and considering the second closed loop, switch SW14, which has the smallest current, is opened. This process continues until the last initially open switch S37 is considered for replacement by another open switch. The final structure with open electric switches is {SW7, SW14, SW9, SW32, SW37}.

The initial power loss of the grid was ΔP_initial = 202.698 kW. After applying OBCMM_2, the power loss ΔP(OBCMM_2) = 139.549 kW, representing a reduction of 63.149 kW compared to the initial state, corresponding to a 31.154% decrease. This reduction is also 1.29% greater than that achieved by OBCMM_1. Table 3 presents the detailed current calculation results for branches using OBCMM_2, and Table 4 along with Figures 4.5 and 4.6 show the node voltages after reconfiguration.

Table 3. Current results of calculating branches according to OBCMM_2 (IEEE 33 nodes).

Circulation	**Branch and current, respectively**							**Open lock**
1	Branch	**2**	**3**	**4**	**5**	**6**	**7**	**SW7**
	Current(A)	146.38	93.75	87.05	83.93	22.26	14.44	
	Branch	**33**	**20**	**19**	**18**			

International Journal of Engineering Research & Technology (IJERT)
ISSN: 2278-0181
Vol. 15 Issue 04 , April - 2026

	Current(A)	38.92	47.76	52.20	56.60			
2	Branch	**9**	**10**	**11**	**12**	**13**	**14**	**SW14**
	Current(A)	16.85	13.82	11.27	7.98	4.76	3.26	
	Branch	**34**						
	Current(A)	15.98						
3	Branch	**8**	**9**	**10**	**11**	**35**	**21**	**SW9**
	Current(A)	15.11	1.61	4.51	6.93	20.23	24.84	
	Branch	**33**						
	Current(A)	25.65						
4	Branch	**2**	**3**	**4**	**5**	**25**	**26**	**SW32**
	Current(A)	132.85	80.47	73.78	70.69	57.50	54.56	
	Branch	**27**	**28**	**29**	**30**	**31**	**32**	
	Current(A)	51.62	48.83	42.30	20.96	14.07	8.86	
	Branch	**36**	**17**	**16**	**15**	**34**	**8**	
	Current(A)	10.10	12.6	14.61	16.93	19.07	21.72	
	Branch	**33**	**20**	**19**	**18**			
	Current(A)	31.98	59.87	64.40	68.86			
5	Branch	**3**	**4**	**5**	**25**	**26**	**27**	**SW37**
	Current(A)	57.91	51.22	48.13	35.01	32.10	29.21	
	Branch	**28**	**37**	**24**	**23**	**22**		
	Current(A)	26.51	25.26	45.47	66.67	71.41		

International Journal of Engineering Research & Technology (IJERT)
ISSN: 2278-0181
Vol. 15 Issue 04 , April - 2026

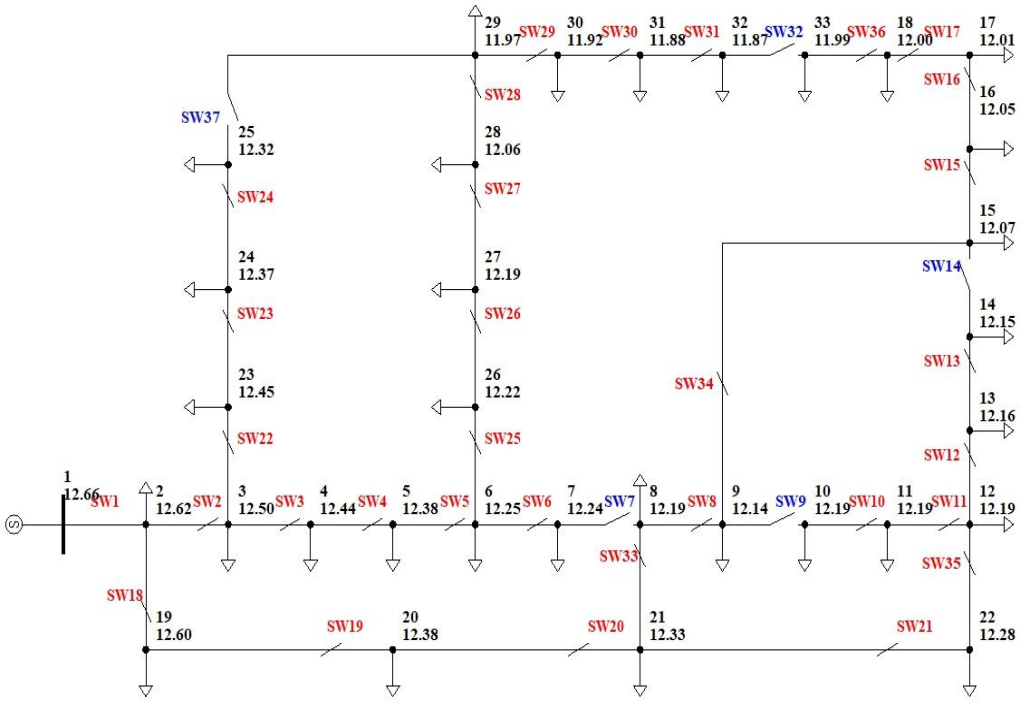

Figure 4.5 Voltage at nodes according to OBCMM_2 (IEEE 33 nodes).

Table 4. Voltage amplitude values of OBCMM_2 nodes (IEEE 33 nodes)

Node	Voltage (kV)	Node	Voltage (kV)	Node	Voltage (kV)	Node	Voltage (kV)
1	12.66	10	12.19	18	12.00	26	12.22
2	12.62	11	12.19	19	12.60	27	12.19
3	12.50	12	12.19	20	12.38	28	12.06
4	12.44	13	12.16	21	12.33	29	11.97
5	12.38	14	12.15	22	12.28	30	11.92
6	12.25	15	12.07	23	12.45	31	11.88
7	12.24	16	12.05	24	12.37	32	11.87
8	12.19	17	12.01	25	12.32	33	11.99
9	12.14						

International Journal of Engineering Research & Technology (IJERT)
ISSN: 2278-0181
Vol. 15 Issue 04 , April - 2026

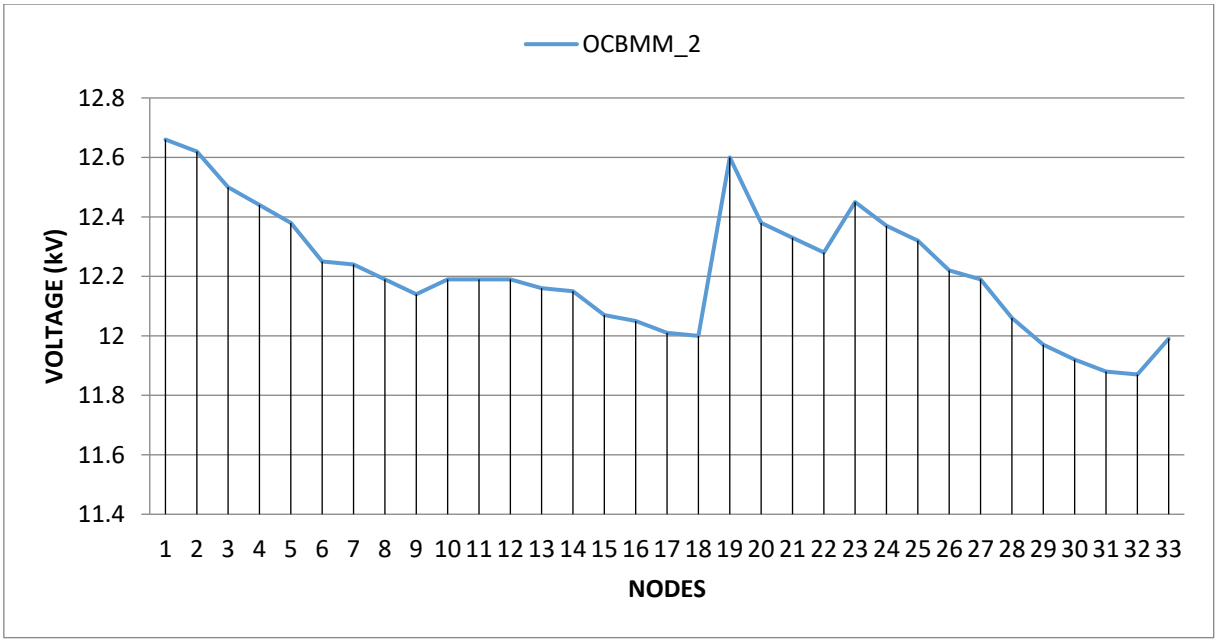

Figure 4.6 Voltage diagram of nodes after restructuring OBCMM_2 (IEEE 33 nodes).

4.1.3. TOPO method (IEEE 33 nodes)

The TOPO method yielded a power loss of 139.549 kW, representing a reduction of 63.149 kW compared to the initial value, equivalent to 31.154%. Table 5 along with Figures 4.7 and 4.8 present the node voltages after implementing TOPO.

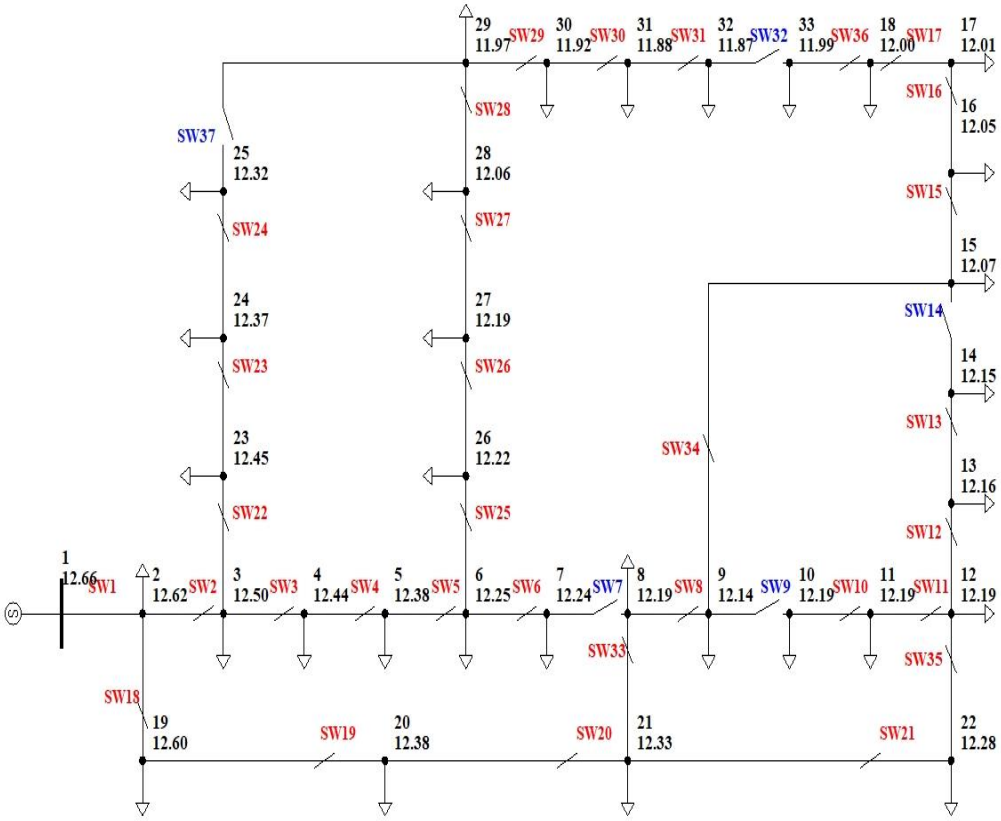

Figure 4.7 Voltage at nodes after performing TOPO (IEEE 33 nodes)

International Journal of Engineering Research & Technology (IJERT)
ISSN: 2278-0181
Vol. 15 Issue 04 , April - 2026

Table 5. Voltage amplitude values at nodes after performing TOPO (IEEE 33 nodes)

Node	Voltage (kV)	Node	Voltage (kV)	Node	Voltage (kV)	Node	Voltage (kV)
1	12.66	10	12.19	18	12.00	26	12.22
2	12.62	11	12.19	19	12.60	27	12.19
3	12.50	12	12.19	20	12.38	28	12.06
4	12.44	13	12.16	21	12.33	29	11.97
5	12.38	14	12.15	22	12.28	30	11.92
6	12.25	15	12.07	23	12.45	31	11.88
7	12.24	16	12.05	24	12.37	32	11.87
8	12.19	17	12.01	25	12.32	33	11.99
9	12.14						

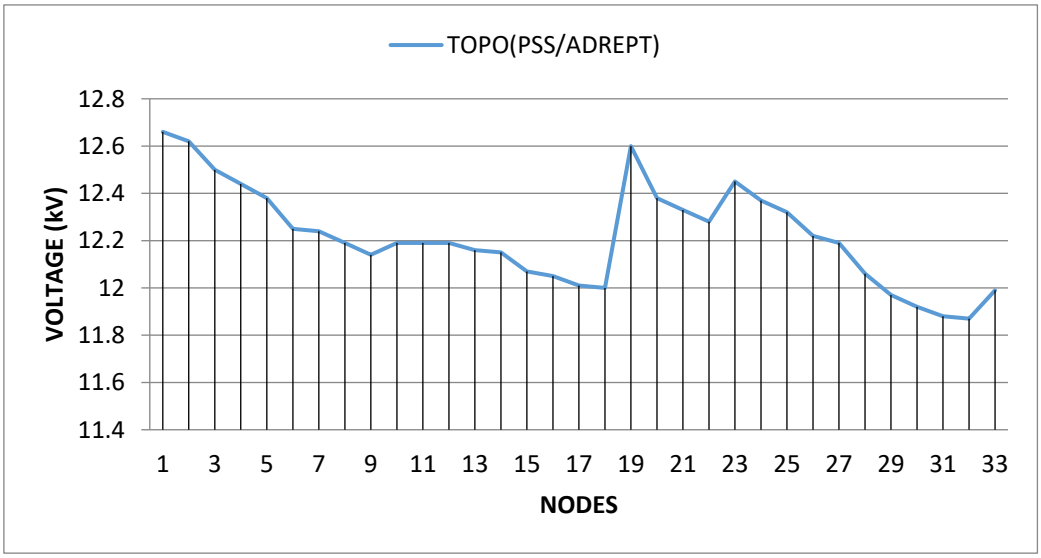

Figure 4.8 Voltage graph at nodes after performing TOPO (IEEE 33 nodes)

The results show that: The power loss is 139,549 kW, down from the initial value of 63,149kW (equivalent to 31.154%). The OBCMM_1 method has a higher loss than the TOPO method at 2,614kW (corresponding to 1,281%), the location of the open keys is almost the same as the TOPO method. The OBCMM_2 method has results comparable to those from TOPO.

4.1.4. Comparative Performance Analysis (Voltage Profile and Power Loss - IEEE 33 nodes).

The node voltage profiles (Figures 4.9, 4.10, 4.11, 4.12) indicate that the voltage values obtained using both OBCMM_1 and OBCMM_2 methods exhibit reduced voltage drops compared to the initial pre-reconfiguration grid, and the voltages closely approximate the results achieved by TOPO. Table 6 summarizes the comparison of optimal configuration selection results regarding power loss:

International Journal of Engineering Research & Technology (IJERT)
ISSN: 2278-0181
Vol. 15 Issue 04 , April - 2026

Table 6. Comparison of optimal configuration selection results (IEEE 33 nodes)

Methods	**Lock open**	ΔP_{Losses} **(kW)**	**Decrease ΔP (kW) compared to the Initial**	**Decrease rate (%)**
Initial	SW33, SW34, SW35, SW36, SW37	202.698	-	-
OBCMM_1	SW7, SW9, SW14, SW36, SW37	142.163	60.535	29.86
OBCMM_2	SW7, SW14, SW9, SW32, SW37	139.549	63.149	31.15
TOPO	SW7, SW14, SW9, SW32, SW37	139.549	63.149	31.15

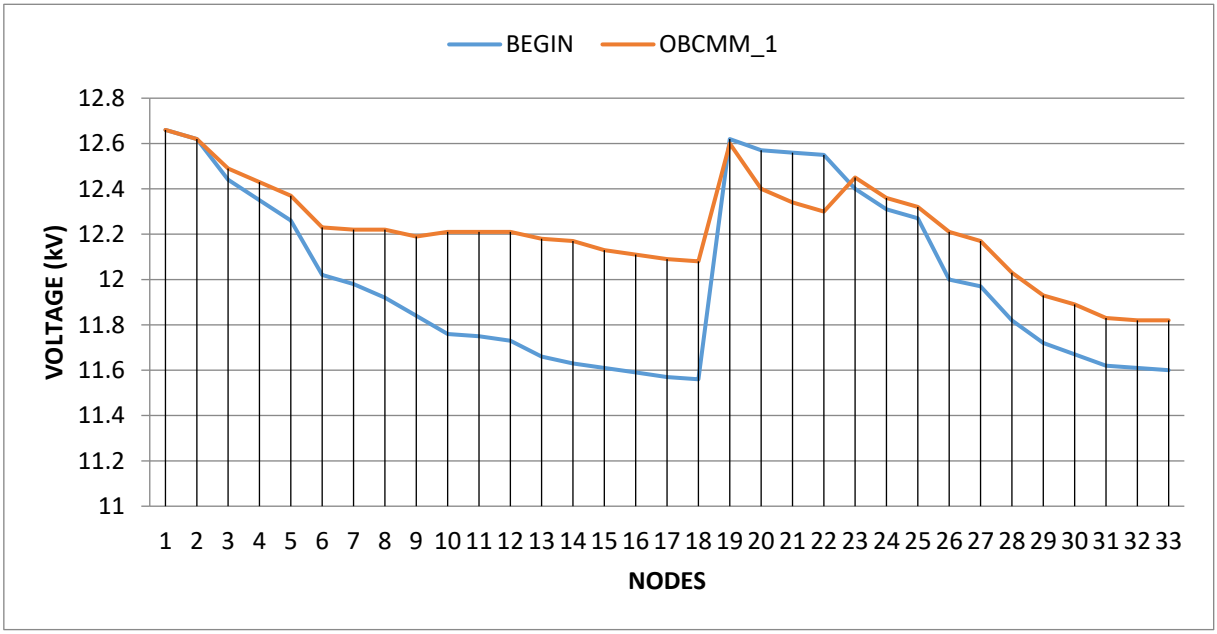

Figure 4.9 Initial grid compared with OBCMM_ 1 method (IEEE 33 nodes)

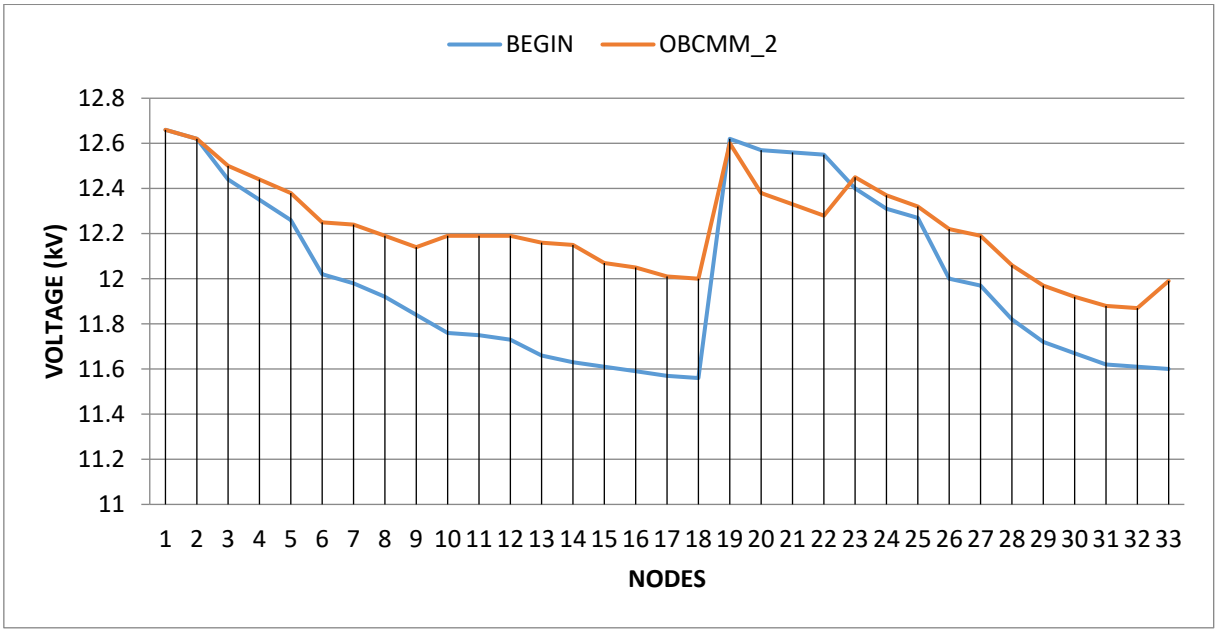

Figure 4.10 Initial grid compared with OBCMM_ 2 method (IEEE 33 nodes)

International Journal of Engineering Research & Technology (IJERT)
ISSN: 2278-0181
Vol. 15 Issue 04 , April - 2026

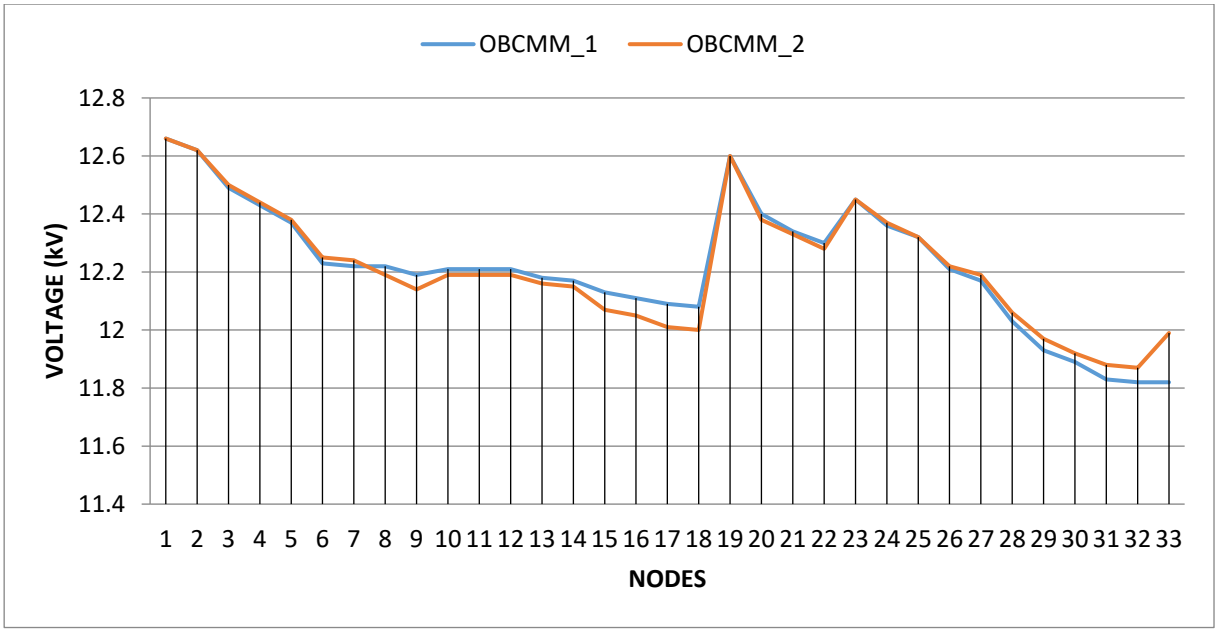

Figure 4.11 Node voltage OBCMM_ 1 compared with OBCMM_ 2 (IEEE 33 nodes)

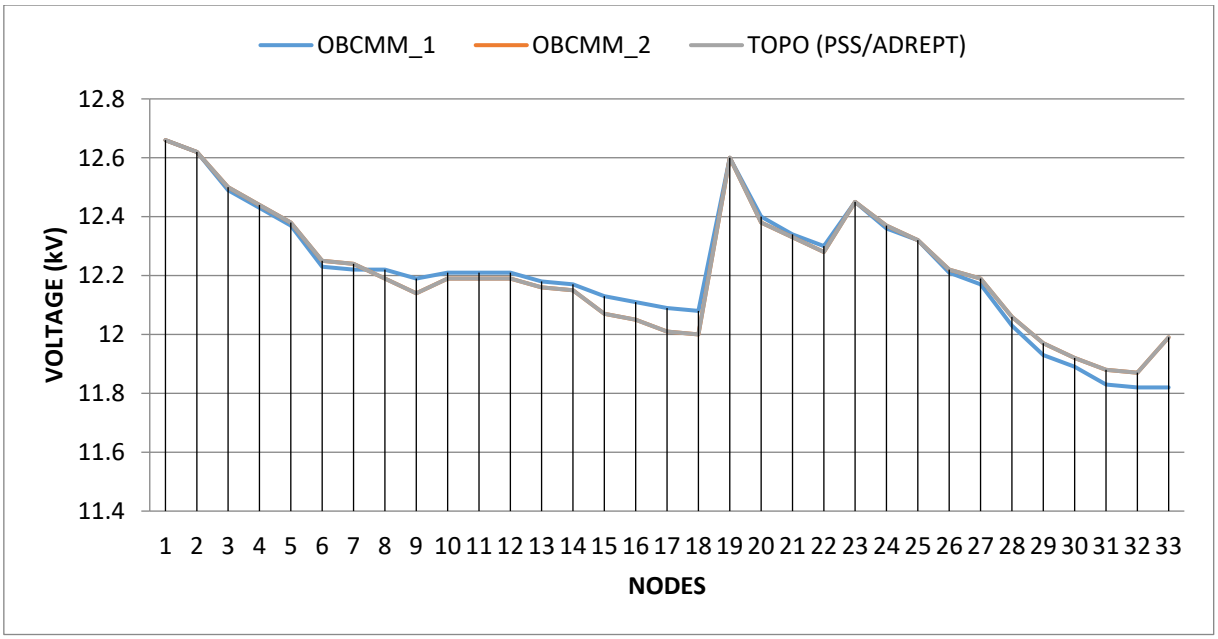

Figure 4.12 Node voltage OBCMM_ 1 and OBCMM_ 2 compared with TOPO (IEEE 33 nodes)

4.2. IEEE 69-Node Distribution Grid

System Parameters and Simulation Setup: The IEEE 69-node distribution grid has a source voltage of 12.66kV. The total active load power is P = 3801.49 kW, and the total reactive load power is Q = 2694.1 kVar. The circuit comprises 69 nodes, 73 branches in total, 68 normally closed switches, and 5 initially normally open switches: S69, S70, S71, S72, S73. The grid diagram is illustrated in Figure 4.13 and simulated using PSS/ADEPT 5.0 in Figure 4.14. Both methods were implemented in PSS/ADEPT 5.0 software to select the optimal operating structure.

International Journal of Engineering Research & Technology (IJERT)
ISSN: 2278-0181
Vol. 15 Issue 04 , April - 2026

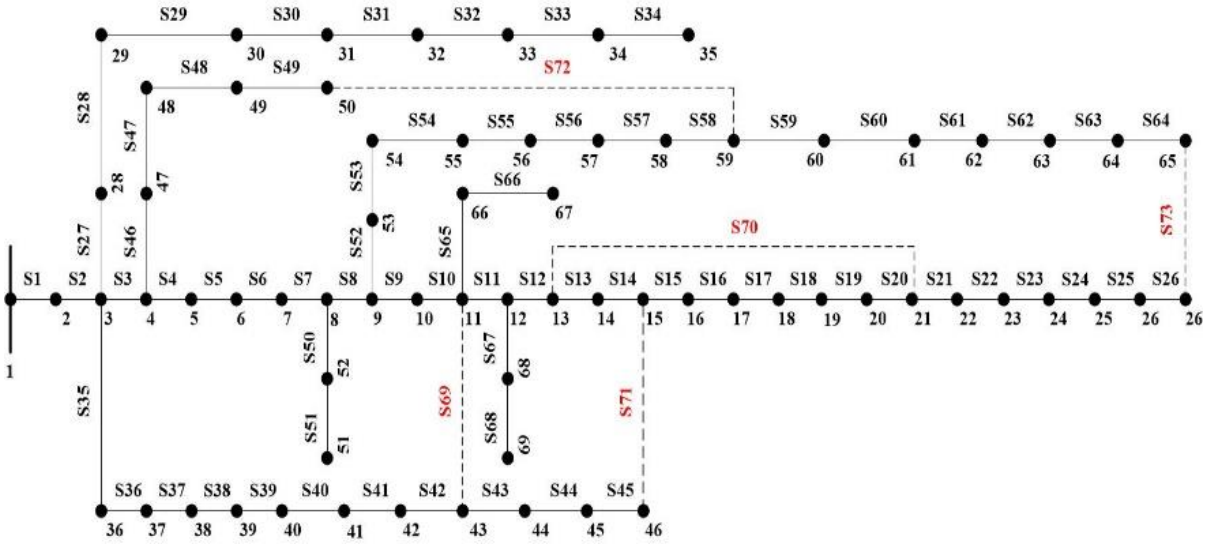

Figure 4.13 DG diagram 69 nodes – original IEEE

Initial Power Loss (IEEE 69 nodes): With the initial switches (S69, S70, S71, S72, S73) in the open state, the initial active power loss of the grid was ΔPLosses = 224.882 kW.

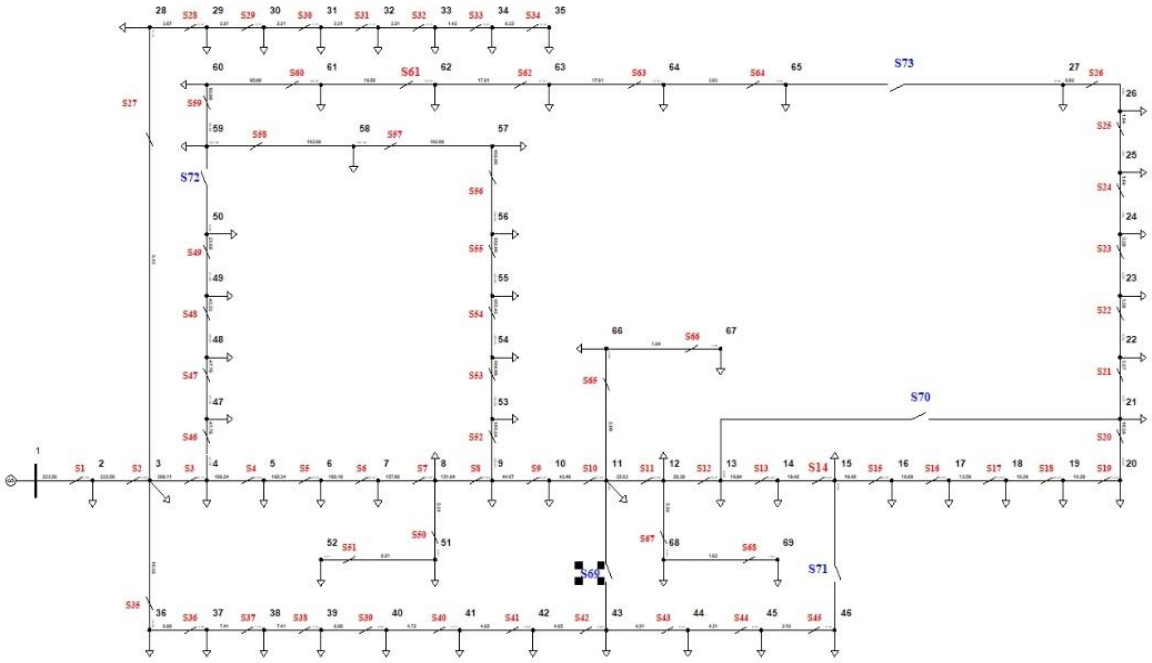

Figure 4.14 IEEE 69 nodes diagram calculated with PSS/ADEPT 5 software.

4.2.1. Evaluation Results

Application of OBCMM_1 Method (IEEE 69 nodes): The results of the OBCMM_1 method show an active power loss of 98.679 kW. This corresponds to a reduction of 126.203 kW compared to the initial grid, achieving a 56.12% reduction. The results of OBCMM_1 are very close to those of TOPO regarding power loss and the sequence of open switches.

Application of OBCMM_2 Method (IEEE 69 nodes): The OBCMM_2 method yielded an active power loss of 108.459 kW. The reduction in power loss compared to the initial grid was 116.423 kW, corresponding to 51.77%. Compared to OBCMM_1, the losses from OBCMM_2 were 4.35% higher. Compared to TOPO, OBCMM_2 yielded results 9.873 kW higher (9.1%).

International Journal of Engineering Research & Technology (IJERT)
ISSN: 2278-0181
Vol. 15 Issue 04 , April - 2026

4.2.2. Comparative Performance Analysis (Voltage Profile and Power Loss - IEEE 69 nodes).

The node voltage profiles (Figures 4.15, 4.16, 4.17, 4.18) demonstrate that the voltage values obtained using both OBCMM_1 and OBCMM_2 methods exhibit reduced voltage drops compared to the initial pre-reconfiguration grid, and the voltages closely approximate the results achieved by TOPO. Table 7 summarizes the comparison of optimal configuration selection results regarding power loss:

Table 7. Comparison of optimal configuration selection results (IEEE 69 nodes)

Methods	**Lock open**	**ΔP_{Losses} (kW)**	**Decrease ΔP compared to the Initial (kW)**	**Decrease rate (%)**
Initial	S69, S70, S71, S72, S73	224.882	-	-
OBCMM_1	S69, S13, S70, S61, S56	98.679	126.203	56.12
OBCMM_2	S10, S17, S12, S56, S61	108.459	116.423	51.77
TOPO	S69, S14, S70, S61, S56	98.586	126.296	56.16

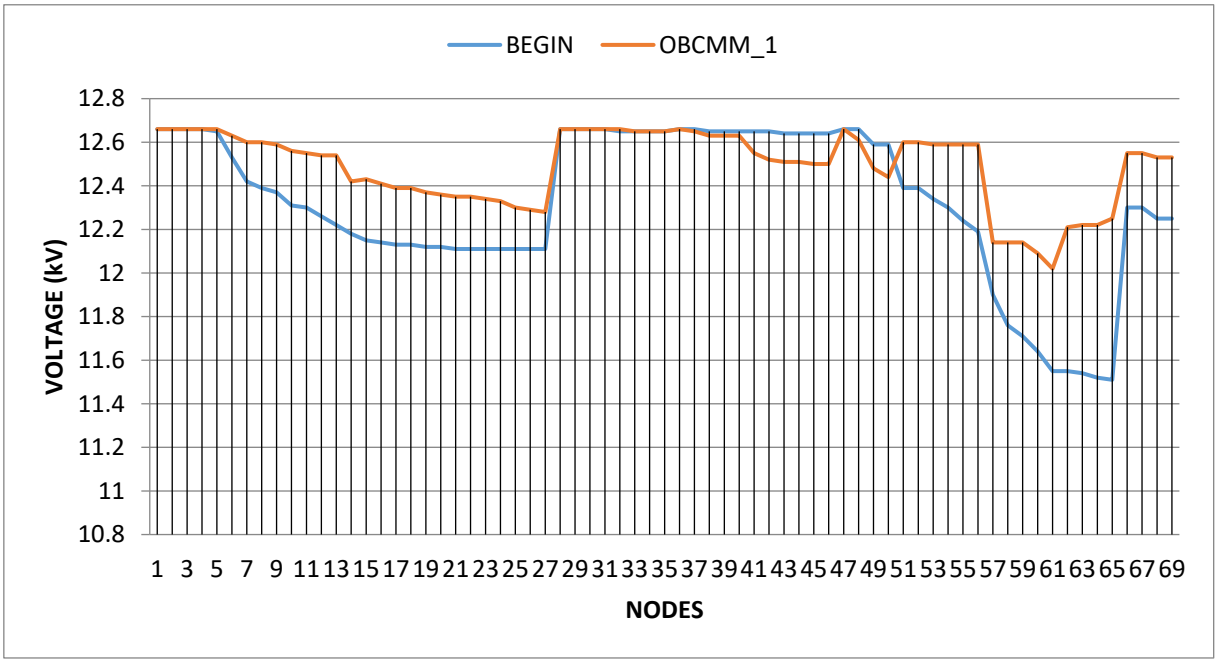

Figure 4.15 Voltage of OBCMM _1 node compared with original grid (IEEE 69 nodes)

International Journal of Engineering Research & Technology (IJERT)
ISSN: 2278-0181
Vol. 15 Issue 04 , April - 2026

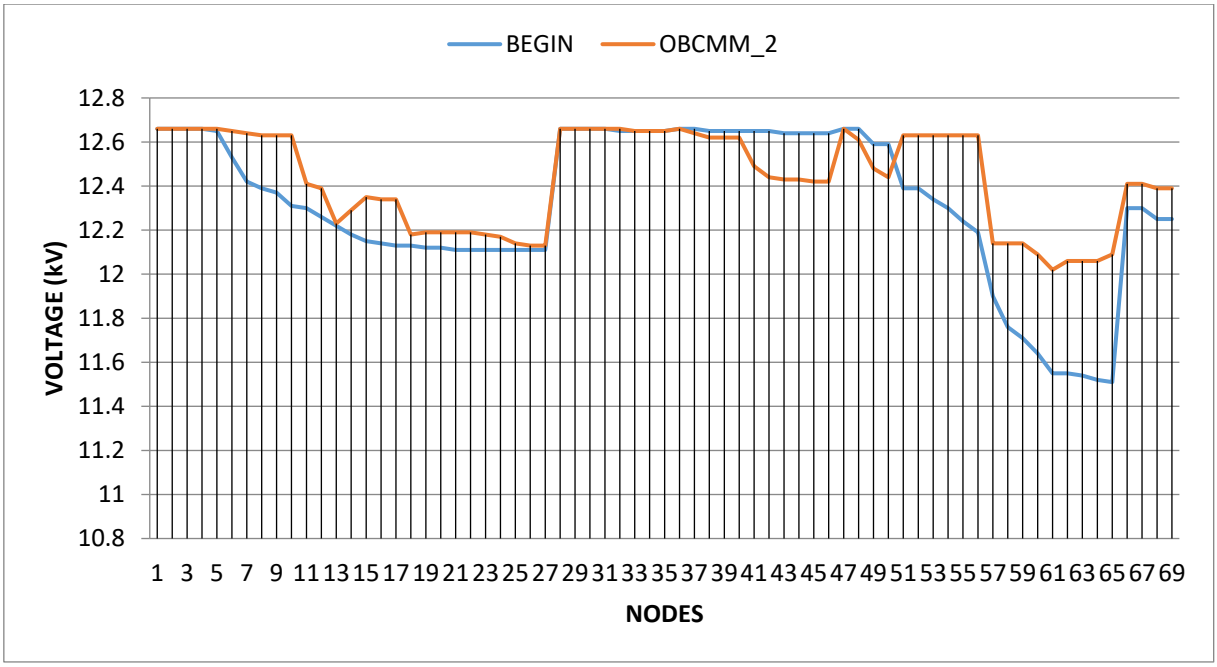

Figure 4.16 Node voltage OBCMM _2 compared with original grid (IEEE 69 nodes)

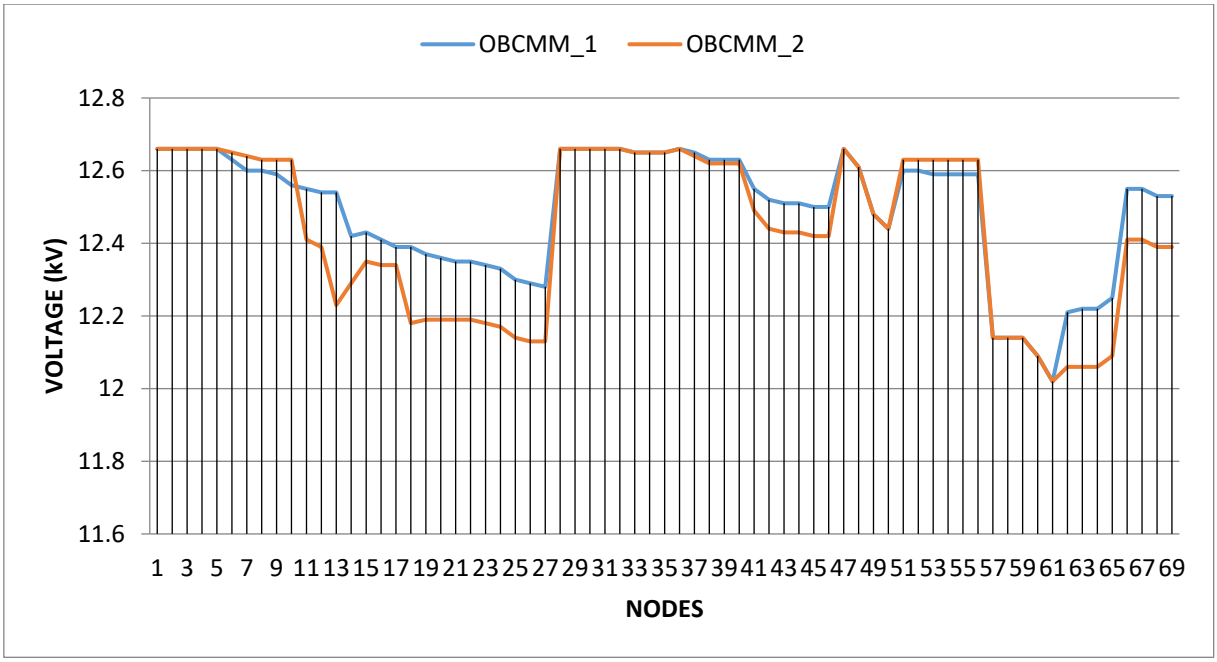

Figure 4.17 OBCMM_1 node voltage compared with OBCMM_2

International Journal of Engineering Research & Technology (IJERT)
ISSN: 2278-0181
Vol. 15 Issue 04 , April - 2026

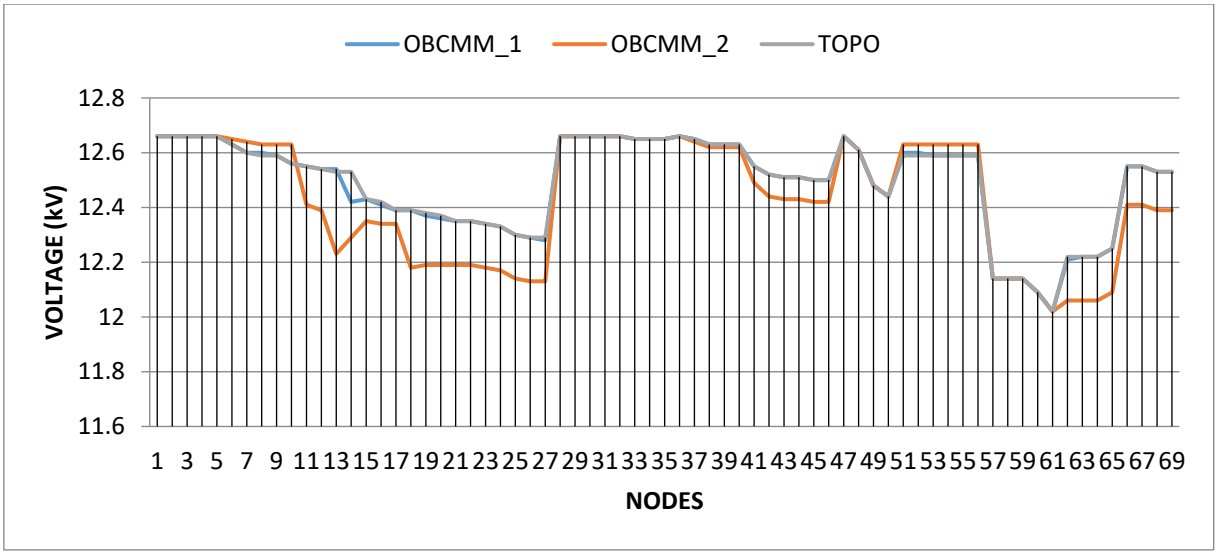

Figure 4.18 Node voltage OBCMM_ 1 and OBCMM_ 2 TOPO comparison (IEEE 69 nodes)

For the IEEE 69-node distribution grid, both OBCMM_1 and OBCMM_2 methods yielded power loss reductions compared to the initial grid. However, the OBCMM_1 method achieved a higher power loss reduction and its results were consistent with the TOPO method.

The reversal in performance dominance (OBCMM_1 performing better for IEEE 69, OBCMM_2 for IEEE 33) is a significant finding. This suggests that as grid complexity (number of nodes, branches, potential loops) increases, OBCMM_1's approach of initially considering all loops and then systematically breaking them may become more robust or effective in finding a near-optimal solution. Conversely, OBCMM_2's sequential, single-loop optimization might be more sensitive to the order of operations in larger, more complex systems, where a suboptimal initial choice could lead to a less efficient final configuration that is difficult to rectify through subsequent steps. This indicates that OBCMM_1, despite its theoretical disadvantage regarding inter-loop influence, may offer a more robust path to near-optimality in larger, more complex networks, while OBCMM_2's strength lies in smaller, less complex systems where its isolated loop optimization can converge precisely. This is a crucial nuance for practical application.

5. CONCLUSION

This paper has meticulously detailed the application of two techniques for selecting the optimal operating structure of distribution grids, based on the optimal branch current model methods (OBCMM_1 and OBCMM_2) and the TOPO algorithm. These methods were employed to operate the IEEE 33-node and IEEE 69-node distribution grids.

The results unequivocally demonstrate that both OBCMM_1 and OBCMM_2 methods are effective in reducing power losses compared to the initial grid configuration, while simultaneously achieving a significant reduction in voltage drop at the nodes. However, the relative performance between these two methods varies depending on the scale and characteristics of the power grid:

- For the IEEE 33-node grid: The OBCMM_2 method yielded a power loss reduction 1.29% greater than OBCMM_1, and its results coincided exactly with those of TOPO. This suggests that for smaller-scale power grids, the OBCMM_2 method can achieve optimal performance, comparable to the benchmark method.

- For the IEEE 69-node grid: The OBCMM_1 method achieved a power loss reduction 4.35% higher than OBCMM_2, and its results regarding open points and power loss were similar to TOPO. This indicates that for larger and more complex power grids, the OBCMM_1 method may be more suitable for identifying an optimal solution.

This conclusion highlights the context-dependency of the two methods' performance. It implies that there is no single "best" method applicable to all scenarios; instead, the optimal choice depends on the specific characteristics (e.g., size, complexity) of the distribution grid. This has significant practical implications for grid operators.

Future research will concentrate on analyzing the impact of the switch opening sequence on the OBCMM_1 method and the impact of the switch closing sequence on the OBCMM_2 method. This endeavor aims to propose more appropriate solutions for distribution

International Journal of Engineering Research & Technology (IJERT)
ISSN: 2278-0181
Vol. 15 Issue 04 , April - 2026

grid operation. This research direction directly addresses the identified disadvantages of each method (inter-loop influence for OBCMM_1, dependence on initial order for OBCMM_2). This demonstrates the authors' commitment to improving the robustness and reducing the sensitivity of these heuristics to initial conditions or operational sequences, moving towards solutions with higher practical applicability.

REFERENCES

[1] Hồ Đắc Lộc. "Ứng dụng giải thuật di truyền tái cấu trúc lưới điện," Tạp chí phát triển KH&CN. Số K2, tr 17–26, tháng 12/2012.
[2] Trương Việt Anh và Nguyễn Tùng Linh. "Đề xuất phương pháp tái cấu hình lưới điện phân phối nâng cao độ tin cậy cung điện," Tạp trí khoa học và công nghệ. Số 3, tr 3–8, tháng 6/2021.
[3] Bạch Quốc Khánh và Nguyễn Văn Minh. "Một số trường hợp đánh giá tổn thất điện năng trong hệ thống cung cấp điện tòa nhà bị ô nhiễm sóng hài," Tạp trí khoa học và công nghệ. Số 42, tr 8 - 11, tháng 10/2017
[4] Trương Việt Anh và các cộng sự. "Tái cấu hình lưới điện phân phối có tải không cân bằng với hàm mục tiêu giảm tổn thất công suất," Tạp chí khoa học và công nghệ năng lượng. Số 21, tr 49–59, tháng 12/ 2019.
[5] Tôn Ngọc Triều và các cộng sự. "Áp dụng phương pháp Backward / Forward cải tiến trong bài toán tối ưu lưới điện phân phối có kết nối nguồn điện phân tán," Tạp chí Phát triển Khoa học và Công nghệ. Số 2, tr 105–115, tháng 8/2019.
[6] T. Thanh Nguyen et al. "Optimal Network Reconfiguration to Reduce Power Loss Using an Initial Searching Point for Continuous Genetic Algorithm," Complexity. Vol 2020, pp. 1 - 21, 2020.
[7] R. J. Sarfi et al. "Distribution feeder reconfiguration for loss reduction," Electr. Power Syst. Res. Vol. 31, no. 1, pp. 61–70, 1994.
[8] S. Civanlar et al. "Distribution feeder reconfiguration for loss reduction," Cell Tissue Res. Vol. 298, no. 2, pp. 1217–1223, 1999.
[9] R. Taleski and Draji "Energy summation method for energy loss computation in radial distribution networks," IEEE Trans. Power Syst. Vol. 11, no. 2, pp. 1104–1111, 1996.
[10] D. Shirmohammadi and H. W. Hong. "Reconfiguration of electric distribution networks for resistive current losses reduction," IEEE Trans. Power Deliv. Vol. 4, no. 2, pp. 1492–1498, 1989.
[11] S. K. Basu. "A new algorithm for the reconfiguration of distribution feeders for loss minimization," IEEE Transactionson Power Delivery. Vol. 7, no. 3, pp. 1484–1491, 1992.
[12] C. S. Chen and M. Y. Cho. "Energy loss reduction by critical switches," IEEE Trans. Power Deliv. Vol. 8, no. 3, pp. 1246–1253, 1993.
[13] R. P. Broadwater et al. "Time varying load analysis to reduce distribution losses through reconfiguration," IEEE Trans. Power Deliv. Vol. 8, no. 1, pp. 294–300, 1993.
[14] J. Mendoza et al. "Minimal loss reconfiguration using genetic algorithms with restricted population and addressed operators: Real application," IEEE Trans. Power Syst. Vol. 21, no. 2, pp. 948–954, 2006.
[15] P. Subbura et al. "Distribution System Reconfiguration for Loss Reduction using Genetic Algorithm," J. Electr. Syst. Vol. 2, no. 4, pp. 1–6, 2006.
[16] D. Jakus et al. "Optimal reconfiguration of distribution networks using hybrid heuristic-genetic algorithm," Energies. Vol. 13, no. 7, 2020.
[17] L. Li and C. Xuefeng. "Distribution Network Reconfiguration Based on Niche Binary Particle Swarm Optimization Algorithm," Energy Procedia. Vol. 17, pp. 178–182, 2012.
[18] J. Olamaei et al. "Application of particle swarm optimization for distribution feeder reconfiguration considering distributed generators," Appl. Math. Comput. Vol. 201, no. 1–2, pp. 575–586, 2008.
[19] S. Sivanagaraju et al. "Discrete particle swarm optimization to network reconfiguration for loss reduction and load balancing," Electr. Power Components Syst. Vol. 36, no. 5, pp. 513–524, 2008.
[20] A. A. Firdaus et al. "Distribution network reconfiguration using binary particle swarm optimization to minimize losses and decrease voltage stability index," Bull. Electr. Eng. Informatics. Vol. 7, no. 4, pp. 514–521, 2018.
[21] F. Sayadi et al. "Feeder reconfiguration and capacitor allocation in the presence of non-currentar loads using new P-PSO algorithm," IET Gener. Transm. Distrib. Vol. 10, no. 10, pp. 2316–2326, 2016.
[22] S. Tiwari and A. Kumar. "Reconfiguration and Optimal Micro-Phasor Unit Placement in a Distribution System Using Taguchi-Binary Particle Swarm Optimization," Arab. J. Sci. Eng., vol. 46, no. 2, pp. 1213–1223, 2021.
[23] P. Siano and D. Sarno. "Assessing the benefits of residential demand response in a real time distribution energy market," Appl. Energy. Vol. 161, pp. 533–551, 2016.
[24] H. F. Zhai et al. "Dynamic reconfiguration of three-phase unbalanced distribution networks," Int. J. Electr. Power Energy Syst. Vol. 99, no. December 2017, pp. 1–10, 2018.
[25] W. C. Wu and M. S. Tsai. "Application of enhanced integer coded particle swarm optimization for distribution system feeder reconfiguration," IEEE Trans. Power Syst. Vol. 26, no. 3, pp. 1591–1599, 2011.
[26] M. A. Kashem et al. "Artificial neural network approach to network reconfiguration for loss minimization in distribution networks," Int. J. Electr. Power Energy Syst. Vol. 20, no. 4, pp. 247–258, 1998.
[27] R. A. Jabr et al. "Minimum loss network reconfiguration using mixed-integer convex programming," IEEE Trans. Power Syst. Vol. 27, no. 2, pp. 1106–1115, 2012.
[28] J. A. Taylor and F. S. Hover. "Convex models of distribution system reconfiguration," IEEE Trans. Power Syst. Vol. 27, no. 3, pp. 1407–1413, 2012.
[29] T.V.Anh et al. "Two states for optimal position and capacity of distributed generators considering network reconfiguration for power loss minimization based on runner root algorithm," Energies. Vol. 12, no. 1, 2019.
[30] G. Merlin and Back. "Search for a minimal - loss operating spanning tree configuration in an urban power distribution system," in Of the Fith Power System Conference. Vol. 1, pp. 1–18, 1975.